Rotational Cation Dynamics in Metal-Halide Perovskites: Effect on Phonons and Material Properties

*Nathaniel P. Gallop[a], Oleg Selig[b], Giulia Giubertoni[b], Huib J. Bakker[b], Yves L.A. Rezus[b], Jarvist Frost[c], Thomas L.C. Jansen[d], Robert Lovrincic[e], Artem A. Bakulin[a]**

[a:] *Ultrafast Optoelectronics Group, Department of Chemistry, Imperial College London, London, SW7 2AZ, UK.*

[b:] *AMOLF, Science Park 104, 1098 XG Amsterdam, The Netherlands.*

[c:] *Department of Physics, Kings College London, London, WC2R 2LS, UK.*

[d:] *University of Groningen, Zernike Institute for Advanced Materials, Nijenborgh 4, 9747 AG Groningen, The Netherlands.*

[e:] *Institute for High-Frequency Technology, TU Braunschweig, Schleinitzstrasse 22, 38106Braunschweig, Germany.*

Abstract

The dynamics of organic cations in metal-halide hybrid perovskites (MHPs) have been investigated using numerous experimental and computational techniques, due to their suspected effects on the properties of MHPs. In this Perspective, we summarise and reconcile key findings, as well as present new data, to synthesise a unified understanding of the dynamics of the cations. We conclude that theory and experiment collectively paint a relatively complete picture of rotational dynamics within MHPs. This picture is then used to discuss the consequences of structural dynamics for electron-phonon interactions, and their effect on material properties by providing a brief account of key studies that correlate cation dynamics with the dynamics of the inorganic sub-lattice and overall device properties.

Metal halide perovskites (MHPs) are enjoying considerable academic and industrial interest due to their high photovoltaic power conversion efficiencies (22% as of July 2017)[1], ease and low cost of production, and broad material tuneability[2]. Besides applications in photovoltaics, MHPs may find use as solar thermoelectric materials[3], LEDs, Lasers[4], and non-volatile memory[5].

The macroscopic properties of MHPs emerge from diverse microscopic phenomena, including crystal structure[6], defects, cation disorder[7], ion migration[8], and spin-orbit coupling[9]. Linking these phenomena to macroscopic performance is challenging due to the complex interplay between them. In this perspective, we will address cation dynamics, their interactions with lattice vibrations (phonons), and their hypothesised effects on device performance.

MHPs share a common ABX_3 (perovskite) structure as shown in Fig. 1. This consists of: (A) an organic molecule (*e.g:* methylammonium (MA), or formamidinium (FA)) or a large inorganic atom (*e.g.:* Caesium), (B) a metal dication (*e.g.*: $Pb^{(II)}$, $Sn^{(II)}$) and, (X) halide anions (Cl, Br, I, or some combination thereof). The M and X species form a corner-sharing octahedral framework. The charge-balancing A-site cation occupies the central cavity generated by this framework and has a strong effect on the MHP structure, quantified by the Goldschmidt Tolerance Factor[10]. A-site ions just above or below the optimum size may induce tilting of the octahedra within the BX_3 sublattice away from a cubic perovskite. Mixing of ions will lead to inhomogeneity in the local structure, which may result in coupling of cation motion and equilibrium distribution to more complex local lattice dynamics.

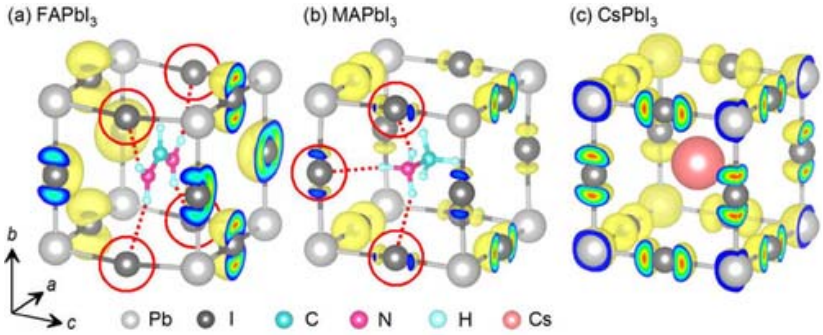

Figure 1: Structures of (a) $MAPbI_3$, (b) $FAPbI_3$, (c) $CsPbI_3$, demonstrating the key interactions between the organic cation and the inorganic sublattice. (Image adapted with permission from Fujiwara *et al.*[11])

Organic cations in MHPs are believed to be rotationally mobile. The extent of rotation varies, from complete immobilisation to facile free-space reorientation, depending on the chemical composition, phase, temperature, pressure, *etc.*[6,12,13] The A-site cation is an essential part of the MHP lattice and their orientations and rotations are likely coupled to the material structure and dynamics. Multiple studies have suggested that cations play a major role in the optoelectronic performance of MHPs. Among the suggested effects are ferroelectricity[14], transport and recombination of polarons[15–17], modulation of phonon density, ion/dopant mobility and other effects.

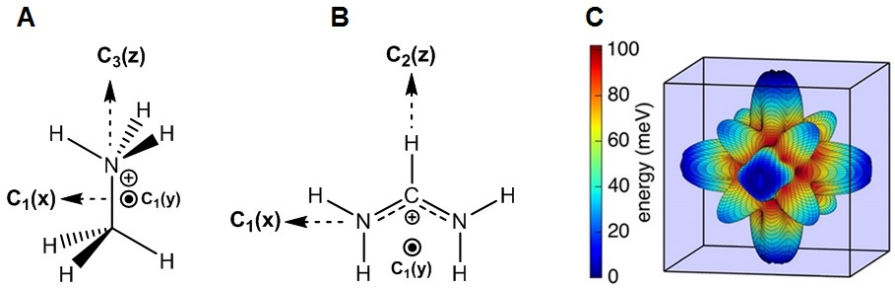

Figure 2: (A) chemical structure of methylammonium, displaying relevant rotational symmetry axes; (B) as in (A) but for FA— highlighting the partial double bond character of the C—N bonds; (C) potential energy surface for orientations of the MA molecule in $MAPbI_3$. (Reproduced with permission from Bechtel *et al.*[18]);

When discussing MA cation motions a distinction should be made between rotation of the C_3 rotational axis containing the C—N Bond, and the 'clicking' rotation of the methyl (or amine) moieties about the C_3 rotational axis (Fig. 2b). We will exclusively discuss C—N axis rotation, which is aligned with the molecular dipole and arguably more relevant to device performance. In FA, rotation about multiple axes must be considered[19]. The 'clicking' rotations found in MA are not present in FA due to its planarity, which arises from the partial double bond character of the FA C—N bonds[20].

A visualisation of the rotational energetic landscape for MA in $MAPbI_3$, computed by Bechtel *et al.,* is provided in Fig. 3c[18]. Global energetic minima exist for cations oriented along the *X* $[100]$ direction, with shallower local minima oriented along the *R* $[111]$ direction. The *X* direction corresponds to the MA lying along the diagonal (most spacious) axis of the octahedral cage, whereas the R direction has the MA bridging two faces of the octahedral[18].

Cation dynamics: Modelling. Numerous computational studies of $MAPbI_3$ and similar lead-halide perovskites[13–15,18,21–30] indicate rotational correlation times of 1-15 ps[13–15,18,25–28] (Table 1), with some predicting immobilisation of the organic cation in the low-temperature orthorhombic phase[13,25,31]. This wide range of values is reflective of the complexity of the problem with differing computer models and approximations capturing different aspects of the dynamics. Additionally, multiple theoretical studies have claimed that cation-cation interaction energies within perovskites may be sufficiently high to facilitate the formation of large domains of aligned cations, leading to ferroelectricity/antiferroelectricity[14,22,32].

Ab initio molecular dynamics (AIMD) simulations directly calculate the electronic structure of the thermally distributed ensemble and are likely to be predictive within the limits of the chosen model. Rotational dynamics of MA in $MAPbI_3$ extracted from AIMD simulations[31] were in good agreement those observed experimentally. A comprehensive summary of AIMD in MHPs is provided by Mattoni *et al.* in a recent review[28]. The high computational cost of AIMD restricts simulations to small systems (10^2—10^3 atoms) over 10—100 ps timescales, meaning that the configurational phase space may not be sampled completely enough to achieve an accurate ensemble average[25] and that long range order cannot be studied. However, a classical empirical force-field molecular dynamics (CMD) study performed by Mattoni *et al.*[13] enabled access to a 4x4x4 (3024 atom) supercell, a 10 ps measurement time, and a 300 ps equilibration time, which allows for better sampling of the phase space. Their results suggest that at 300 K the MA cations rotate freely but become increasingly restricted at lower temperatures to the faces of the PbI_3 octahedral cavity (Fig. 2c). However, the accuracy of these results depends on the properties of the empirical force-field and thus experimental verification is necessary.

A molecular dynamics study accounting for the polarizability of the inorganic ions allowed modelling of 6x6x6 (3456 atom) supercells for 2 ns and reproduced the slowdown of the MA rotation in halide alloys[33].

Cation Dynamics: Steady State Experiments. Cation motion in MHPs has been investigated using numerous techniques, including solid-state NMR (ssNMR)[12,34], dielectric relaxation[7], IR spectroscopy[35], and *Quasi*-Elastic Neutron Scattering[32,36] (QENS). In ssNMR, rotational dynamics are computed from the spin-lattice (T_1) relaxation time, and the ^2H and ^{14}N spectral lineshapes. In QENS, rotational dynamics are inferred from the energy change of incident neutrons due to incoherent scattering from individual hydrogen nuclei[32,36]. In linear IR, the width of suitable spectral lines is used to infer rotational correlation times[35], while in dielectric relaxation studies, the effect of changing temperature on the dielectric constant is fit to a Debye relaxation model[7].

An early dielectric relaxation study by Poglitsch and Weber[7] obtained a rotational correlation time of 5.4 ps in $MAPbI_3$, whilst a contemporaneous ssNMR study performed by Wasylishen *et al.* obtained correlation times of ~0.2-0.5 ps, for $MAPbI_3$ $MAPbBr_3$ and $MAPbCl_3$ at 303 K, with the rotational lifetime increasing in the order Br<Cl<I[34]. A follow-up study by Bernard *et al.*[12] reported similar rotational lifetimes for $MAPbI_3$ at 300 K. Another early study utilised linear IR spectroscopy to estimate a rotational correlation time of ~1 ps for $MAPbI_3$, with correlation times increasing in the same order (Br<Cl<I) at ~300 K[35]. A more recent QENS study by Leguy *et al.* extracted a rotational lifetime of ~14 ps[32], significantly longer than a correlation time of 4.7 ps obtained by Chen *et al.* using the same technique[36]. Chen *et al.* pointed to the limited data range in energy and momentum space used by Leguy *et al*. to explain this discrepancy[36]. Additionally, several studies suggest a phase dependence on cation orientation[12,32]. In all cases, cations are aligned towards the faces of the PbI_3 cage with certain orientations preferred in the low temperature Orthorhombic/Tetragonal phases (Fig. 2C). In the high temperature cubic phase, all faces are equally favoured, and rotations become isotropic.

Cation dynamics: Time-resolved vibrational studies. Recently, polarisation-resolved 2-dimensional IR (2DIR) spectroscopy has been used to observe cation dynamics through measurement of the rotational anisotropy[31,33]. The principle behind a polarisation-resolved pump-probe experiment is displayed in Fig. 3a; a linearly polarised pump pulse (purple), resonant with the C—N stretching mode, is absorbed by a MA cation whose vibrational transition dipole moment ($\vec{\mu}_t$) is parallel to the pump pulse's electric field vector (purple arrow). Some time (τ_{probe}) after the pump pulse, during which the organic cation (and thus $\vec{\mu}_t$) may rotate, a probe pulse with polarisation either orthogonal (orange), or coplanar (blue) to the pump pulse arrives at the molecule. Absorption of the probe pulse is dictated by the angle formed by the electric field of the probe pulse (orange/blue arrow) and the current transition dipole moment vector ($\vec{\mu}_{t+\tau}$). The relative absorption changes between the polarised probe pulses yields the response anisotropy for various τ_{probe} values, which is related to the rotational correlation function of the probed transition dipole. Thus, the dynamics of the vibrational transition dipole can be connected to the cation's various degrees of freedom (Fig. 2b,c).

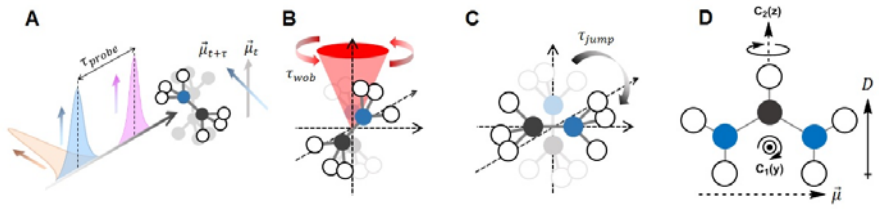

Figure 3: (A) Pulse sequence used in polarisation resolved 2DIR. (B) Modes of rotation in $MAPbI_3$, including 'wobbling within a cone' (top), and C—N axis rotation to an adjacent energetic minimum (bottom). In $FAPbI_3$ (C), these modes may occur along the principal rotational axis, $C_2(z)$, or along the orthogonal $C_1(x)$ axis; (D) structure of $FAPbI_3$, displaying the permanent molecular dipole ($\boldsymbol{D}$), the C—N transition dipole moment ($\vec{\mu}$), and the two rotational axes that reorient $\vec{\mu}$ and so contribute to the anisotropy response.

For MA, the orientation of the symmetric NH_3 bending transition dipole coincides with permanent dipole moment. The anisotropy dynamics of this mode were resolved using 2DIR in $MAPbI_3$ ($MAPbBr_3$, $MAPbCl_3$), and were shown to contain two components with characteristic decay times of ~300 fs and ~3 ps (1.5 ps, 1 ps) respectively[31,33]. These well-resolved decays were also identified in *ab initio* MD simulations and attributed to two separate modes of rotation: a rapid 'wobbling in a cone' motion around a local equilibrium aligned with the crystal axis (Fig. 3b), and a (slower) 'reorientational jump' of the MA C—N axis to an adjacent equilibrium position (Fig. 3c), similar to a model previously proposed by Leguy *et al*[32].

Commented [AB1]: https://www.ncbi.nlm.nih.gov/pmc/articles/PMC1328828/

Time-Resolved Optical Kerr Effect (TR-OKE) spectroscopy has also been used to investigate cation rotation in Br-based MHPs[37]. In TR-OKE, a pump pulse induces a transient birefringence in a sample, which is measured over time with a secondary probe pulse. TR-OKE studies in $MAPbBr_3$ and $FAPbBr_3$ identified three regimes of motion. The intermediate (400-600 fs) and slow (1—2 ps) decay components agree well with the 2DIR data discussed above and, by analogy to TR-OKE studies on liquids[38], are attributed to *"frustrated rotation"*, and *"rotational diffusion"* motions, respectively[37]. "Frustrated rotation", and "rotational diffusion" broadly correspond to the 'wobbling in a cone' and 'reorientational jump' modes discussed in Refs. 28,30 and 37 and displayed in Fig. 2.

A commonly invoked mechanism for the presence of rotational energy barriers that give rise to discrete orientational jumps is the elongation of the $N-H\cdots X$ hydrogen bond beyond its equilibrium position[33,39]. A comparative 2DIR study by Selig *et al.* on MA cation dynamics in systems with different halides found, counterintuitively, that the rate of rotation *increased* in the order $MAPbI_3$→$MAPbBr_3$→$MAPbCl_3$ (*i.e.:* increased with increasing hydrogen bond strength and decreasing octahedral cavity size)[33]. This effect was reproduced in CMD simulation and hypothesised to arise from two effects: (i) a reduction in the energetic penalty for elongation of the $N-H\cdots X$ hydrogen bond that lowers the activation barrier height, and (ii) cation rotation coupling to low-frequency ('tilting mode') PbX_3 phonons that physically reorient cations within the octahedral cavity, the frequency of which increases in the order $MAPbI_3$<$MAPbBr_3$<$MAPbCl_3$[40–42]. The latter argument comes from the observation that a static (frozen octahedral) picture predicts energetic barriers that would be extremely rarely crossed.

A similar 2DIR study of cation rotations in $FAPbI_3$ has also been performed by Taylor *et al*[19]. In this case, the N=C—N antisymmetric stretching vibration was used as a probe for FA rotation. While the transition dipole of this vibration is orthogonal to the permanent molecular dipole (Fig. 3d), it provides a good estimate for molecular reorientation rates. The study also revealed rapid 'wobbling within a cone' of FA about a local minimum, along with slower reorientational jumps between adjacent lattice faces.[19] Rotational correlation times for $FAPbI_3$ (470 ± 50 fs and 2.8 ± 0.5 ps for wobbling and flips, respectively) are similar to those in $MAPbI_3$. These values agree well with the AIMD-derived value of 2.0 ps[20], which also indicated a strong preference for the FA to align with the X axis of the cage. A study by Svane *et al.*, which subtracts the electrostatic contribution from an *ab initio* calculation attributing the reminder to hydrogen-bonding, suggests that the strength of hydrogen bonds in $FAPbI_3$ is about 100—150 meV less than in $MAPbI_3$[43]. A rotation model where energetic barriers are dictated by hydrogen bonding interactions would therefore predict slower rotational rates in $MAPbI_3$, compared to $FAPbI_3$, which contradicts the experimentally observed trend. Similarly, if steric

interactions exclusively dictate rotational energetic barriers, the larger size of FA (compared to MA) would result in slower rotational rates in $FAPbI_3$, compared to $MAPbI_3$.

Anisotropy decay measurements also reveal more complex and inhomogeneous structural dynamics in mixed-halide and mixed-cation perovskites (Fig. 4). A halide substitution study on MA-based perovskites (Fig. 4a) indicated a long-lived component in the anisotropy decay for the mixed-halide systems, $MAPbI_xBr_{3-x}$ and $MAPbBr_xCl_{1-x}$[33]. MD simulations indicated that this long-lived component is present only in a sub-ensemble of unit cells, while many MA cations behave in a similar manner to pure $MAPbX_3$. This implies that the specific cell configurations (and their dynamics) dictate cation rotations. When the unit cell contains a variety of halides, the resulting non-symmetric distribution of X-site anions leads to symmetry breaking of the unit cell, creating an anisotropic potential within the A-site cavity that locks the cation in an energetic minimum.

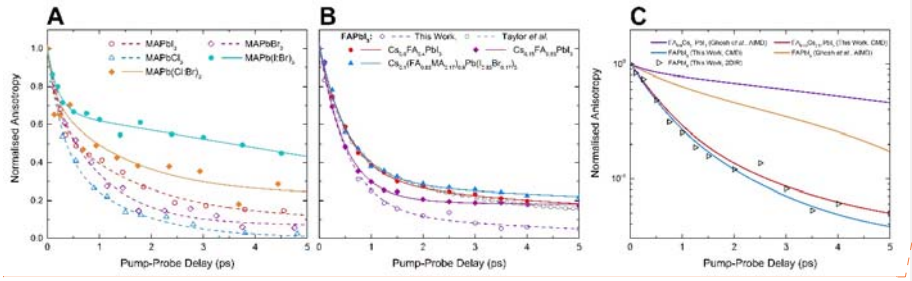

Figure 4: (A) 2DIR transient anisotropy signals for pure (open points) and mixed halide (filled points) MHPs, taken from Selig *et al.*[33]; (B) newly obtained 2DIR anisotropy y decays for mixed cation and mixed cation/halide perovskites (open points, solid lines)— we also include an anisotropy decay curve for pure $FAPbI_3$ obtained by us (purple open circles), as well as a similar curve from Taylor *et al.*[19] for reference; (C) Simulated anisotropy decay curves of $FAPbI_3$ and a mixed FA/CS perovskite. The results of an AIMD study by Ghosh *et al.*[44] (purple/yellow curves) have also been included for comparison. Lines are bi-exponential guides to the eye.

We present new results (Fig. 4b and Fig. 4c (red/blue curves and black triangles)), which indicate that similar effects manifest in perovskite materials containing mixed cation compositions. Fig. 4(b) displays the anisotropy of the C—N antisymmetric stretch in several FA-based perovskite systems. We use the ESA signal in the 1700—1720 cm^{-1} range and apply a thermal response correction (See SI) to probe the true anisotropy dynamics. In MHPs where the A-site cation is solely FA, we observe similar fast rotational dynamics to those observed by Taylor *et al.*[19] albeit with a shorter and less pronounced long-time component. The data for pure perovskites fits well the results of our MD simulations (Fig. 4c, blue and red curves, see SI for details).

The mixed cation perovskites in contrast possess a slow anisotropy decay tail similar (but not as pronounced) to those observed in mixed halide systems (Fig. 4a). An analogous result is seen in the rotational dynamics of FA in the ternary cation MHP $Cs_{0.1}(FA_{0.83}MA_{0.17})_{0.9}Pb(I_{0.83}Br_{0.17})_3$. We also carried out MD simulations (Fig. 4c, blue and red curves) that, whilst able to qualitatively reproduce the slowing down of rotational dynamics upon cation mixing, predict the effect to be very small. Interestingly, the results from AIMD simulations on pure and mixed cation MHPs performed by Ghosh *et al.* in a previous study[44] (Fig. 4c, purple and yellow curves) reproduce the effect of cation mixing much better than our CMD findings, though they appear less precise in capturing the actual timescales of the dynamics. Overall, we can conclude from our results (Figs. 4b,c), as well as those reported

Commented [AB2]: - Rescale panel C to have more space for the legengd
- increase legend and axis notation font
- bolder axes

previously in the literature[19,44], that both experiment and theory agree that cation substitution effects are not completely local but spread beyond the material unit cell. The key mechanism for this is arguably the symmetry breaking in the crystal lattice. The molecular dynamics simulations presented in Fig. 4c assumed an isotropic distribution of the MA and Cs ions, while ion ordering may enhance the observed effect. Furthermore, the agreement with experiment may be improved by tuning the employed Caesium parameters.

A 'Unified' picture of cation dynamics. The rotational time constants obtained using various steady-state and time-resolved methods are displayed in Table 1. Experimental mean correlation times vary between 0.1–8 ps. However, 2DIR and TR-OKE studies provide direct evidence for contemporaneous 'fast' and 'slow' rotations within $MAPbI_3$ and $FAPbI_3$[19,31,33,37]. To demonstrate this, we have grouped various rotational correlation times into 'fast' (300—600 fs) and 'slow' (2—8 ps) categories, neglecting two outliers of 3.1/13.8 ps[32] and 108 ps[45], whose values have been contradicted using identical techniques[12,34,36,46]. We propose that certain experimental techniques may accurately probe one regime of rotational motion but may be less sensitive to the other. We also note that certain techniques (*e.g.:* 2DIR) are sensitive to the second order rotational correlation function, while other techniques (*e.g.:* dielectric light scattering) are predominantly sensitive to the first order correlation function. Surprisingly, though a direct comparison between the constants in such techniques cannot be made, the conclusions of all available experiments can be interpreted within a unified two-timescale picture of cation dynamics.

Recently, an HRTEM study by Zhang *et al*[47] observed the formation of persistent (>1 s) ordered domains of MA at ~300 K (Personal Communication, May 6th 2018). Similar observations of ferroelectricity have also been reported by Röhm *et al*[48]. Whilst it may appear that the observation of ferroelectricity in these two studies contradict earlier reports that claim no ferroelectricity[49–51], we note that the techniques used in these two studies are predominantly sensitive to surfaces or were applied to samples with a large interface contribution, whilst the other methods described previously are bulk sensitive. Thus, there is not necessarily any conflict between the results of Zhang/Röhm *et al.*, and those that suggest a lack of bulk ferroelectricity in MHPs.

These observations of surface ferroelectricity suggest that rotational motion might become 'frozen-out' close to the surface of the MHP because of symmetry breaking. The influence of these surface domains on charge dynamics remains an open question, with at least one study claiming that surface ferroelectricity has a negligible effect on charge separation and transport[52]. Further theoretical and experimental studies are required to ascertain both the prevalence and significance of ferroelectric behaviour within $MAPbI_3$[53].

Table 1. Summary of cation rotational times in different metal halide perovskites at room temperature from different studies with various experimental techniques. All 2DIR studies and one NMR study found two components, summarized as fast and slow.

Study	Ref.	Material	Method	Correlation Time (ps)	
				Fast	Slow
Bakulin et al.	31	$MAPbI_3$	2DIR	0.3	3
Leguy et al.	32	$MAPbI_3$	QENS	3.1	13.8
Chen et al.	36	$MAPbI_3$	QENS	-	4.7
Onoda et al.	35	$MAPbI_3$	Linear IR	~1	-
Poglitsch & Weber	7	$MAPbI_3$	Dielectric Relaxation	-	5.37
Wasylishen et al.	34	$MAPbI_3$	ss-NMR	0.46	-
Bernard et al.	12	$MAPbI_3$	ss-NMR	0.58	1.7 (±0.6)
Fabini et al.	46	$MAPbI_3$	ss-NMR	-	7

Kubicki et al.	[45]	$MAPbI_3$	ss-NMR	-	108 (±0.5)
Taylor et al.	[19]	$FAPbI_3$	2DIR	0.47 (±0.05)	2.8 (±0.5)
Kubicki et al.	[45]	$FAPbI_3$	ss-NMR	-	8.7 (±0.5)
Fabini et al.	[46]	$FAPbI_3$	ss-NMR	-	8
Selig et al.	[33]	$MAPbBr_3$	2DIR	0.3	1.5
Wasylishen et al.	[34]	$MAPbBr_3$	ss-NMR	0.36	
Zhu et al.	[37]	$MAPbBr_3$	TR-OKE	~0.1	~2
Zhu et al.	[37]	$FAPbBr_3$	TR-OKE	~0.1	~2
Selig et al.	[33]	$MAPbCl_3$	2DIR	0.3	1.2
Wasylishen et al.	[34]	$MAPbCl_3$	ss-NMR	0.36	

From these results, a picture of the rotational behaviour of cations within bulk $MAPbI_3$ emerges (figure. 5), in which cationic motion consists both of a rapid 'wobbling' around a local minimum[18,19,31,33], along with slower reorientational 'flips' between adjacent local minima. The reorientation rate is potentially dictated by steric effects, polarizability effects, the characteristics of the cation-halide hydrogen bonds, and coupling to the PbX_3 phonons. In the high temperature (>327 K) cubic phase, the organic cation rotates freely within a symmetric environment. During the cubic-to-tetragonal transition, the lattice distorts along the c direction, creating an anisotropic environment that increasingly constrains cation motion to two dimensions[12,34]. Through the first-order phase transition to the orthorhombic phase, tilting of the inorganic cage wholly stops, resulting in cation motion becoming 'frozen out', with condensation of ferroelectric domains possibly occurring in concert[14,22,32]. When the symmetry of the material is broken by the mixing of different halides/cations (or arguably by proximity to the crystal surface) cation rotation becomes restricted. Some reports indicate that ordered cationic domains persist close to the crystal surface even at relatively high (~300 K) temperatures[47,48].

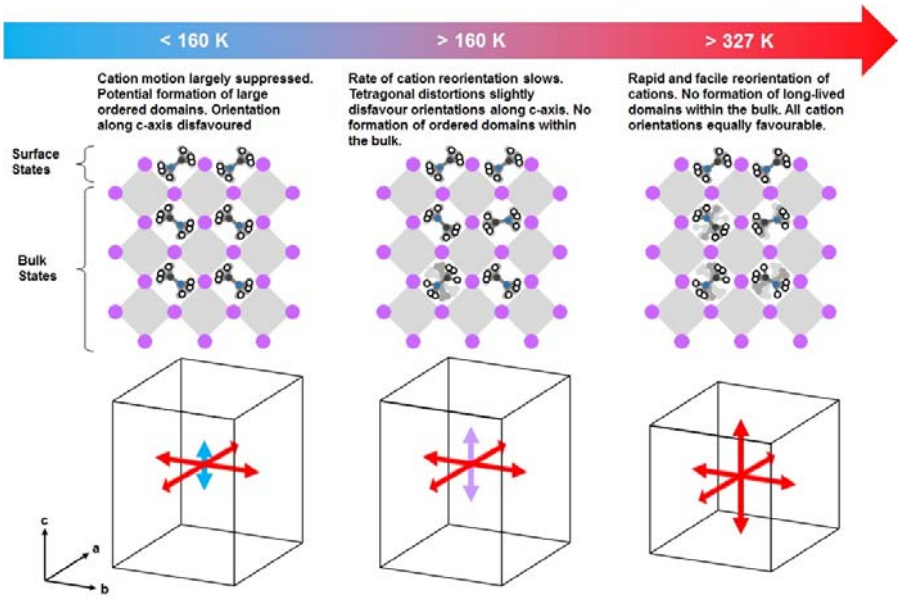

Figure 5: A summary of the rotational dynamics within MAPI. The bottom diagrams (adapted from Ref.[12]) Illustrate the relative likelihood of the methylammonium CN axis orientating itself to a given lattice face, with longer (shorter) arrows indicating an increased (decreased) likelihood. Cartoons demonstrating the dominant rotational modes over a given temperature range are provided in the middle.

Lattice Dynamics. Lattice vibrations (phonons) are expected to be intrinsically coupled to cation rotation and have a significant effect on the properties of MHPs. Vibrations in MHPs containing organic cations can be grouped into three categories[40,54,55]: (i) lattice phonons of the PbX_3 metal-halide cage[41], (ii) internal vibrations of the organic cations[56], and (iii) mixed modes (lattice vibrations coupled with libration/translation of the cation). Internal cation vibrations are readily distinguishable as their energies lie above 100 meV, whereas the lattice vibrations have energies below 20 meV[55]. Such low phonon energies are quite exceptional for inorganic semiconductors and reflect the softness of the material. This softness implies the possibility that the floppy lead halide lattice dynamically reacts to the organic cation reorientations.

The potential impact of cation dynamics on lattice vibrations in MHPs is an important open question. Recent low-energy Raman scattering measurements compared the low energy vibrations in $MAPbBr_3$ and its all-inorganic counterpart, $CsPbBr_3$[57]. When compared in the same crystal phase, the results suggest that the organic cation has a negligible effect on the lattice dynamics in this material class, with strong anharmonicity apparent for both $MAPbBr_3$ and $CsPbBr_3$. This proves that large amplitude anharmonic motions are an inherent characteristic of MHP materials, irrespective of the presence of an organic cation. However, at room temperature, $MAPbBr_3$ clearly exhibits stronger dynamic disorder than $CsPbBr_3$[57]. This implies that at temperatures important for device operation, cation induced structural dynamics of the inorganic lattice may be important. For instance, a comparison of the transverse optical phonons in $MAPbI_3$ and PbI_2 showed greater anharmonicity in $MAPbI_3$[41]. Similarly, a recent study by Kabakova *et al.* found significant differences in the phonon velocities of a variety of MHPs, incorporating differing A-site and X-site cations[58]. Additionally, a recent 2-dimensional terhertz-infrared-visible (2D TIRV) study by Grechko *et al.* directly observed coupling between low frequency

(< 100 cm^{-1}) I—Pb—I phonon modes and N—H stretching modes in both $MAPbI_3$ and $FAPbI_3$[59], suggesting that the dynamics of the organic and inorganic sublattices are strongly coupled. Furthermore, 2D TIRV spectroscopy has directly observed correlations between low frequency inorganic sublattice vibrations and the optical bandgap[60]. This suggests that coupling between the dynamics of the organic and inorganic sublattices are both prevalent and highly relevant to material properties. To fully understand the interplay of cation dynamics and lattice vibrations, further comparative experimental studies of organic and inorganic MHPs will be necessary, together with advanced computational methods that account for hydrogen bond interactions between cations and the inorganic sublattice.

Consequences for Device Performance. Both cation rotations and lattice oscillations are believed to influence the optoelectronic performance of MHPs. It has been proposed that cation rotations play a role in several phenomena, including modulation of the dielectric function[7,61,62], ferroelectricity[14,32], carrier dynamics[15,17,63], and ion transport[64,65], among others. Additionally, phonons within MHPs are thought to play a significant role in the modulation of the optical bandgap, as well as in charge transport[66], exciton dynamics[67], and carrier cooling[41,68,69]. It is important to note that many of these studies lack experimental validation, and thus the significance of cation rotations and their effects on device performance remains an open question.

We first consider the effect of cation reorientation on the migration of ions and ionic defects in MHPs. Ion migration has been implicated as a factor that results in the highly hysteretic current-voltage characteristics typical of perovskite solar cells[8,70,71], although a study by Calado *et al.* observed ion migration even in so-called 'hysteresis free' perovskite solar cells[72]. Ionic hysteresis in MHPs may be useful in memristors and non-volatile memory. Recent a*b initio* MD simulations on MAPI observed a correlation between rotation of the methylammonium cation and migration of an iodide vacancy to an adjacent lattice site[64], although the significance of this effect is unclear. Another model, proposed by Tong *et al,* suggests that ordered dipolar domains enhance ion conduction by reducing the energy barrier for the hopping of negative (positive) charges in directions aligned with (against) the methylammonium dipole[65]. It should be noted however, that the prevalence and significance of ordered dipolar domains remains controversial. Reconciling the existence of ferroelectricity with observation of rapid (~ps) cation rotations remains a significant outstanding hurdle. Huang *et al.* in a recent review suggested that the polarisation-electric field loops reported in multiple studies, which are typically taken as diagnostic of ferroelectricity, may arise from other effects, such as ion migration, current leakage, or back-to-back diodes[73–75]. Additionally, several studies claiming to correct for these effects have been unable to identify ferroelectric behaviour in $MAPbI_3$[49–51]. However, recent observations of surface dipolar domains[47,48] means that cation induced ferroelectricity may alter ionic conductivity with proximity to the surface.

In solar cells, the dielectric function is extremely important, as it directly influences the exciton binding energy. For example, it is now believed that the low exciton binding energies found in $MAPbI_3$ result in direct generation of free charges, as opposed to excitons[73]. In $MAPbI_3$, discontinuities in the low frequency dielectric constant with changing temperature are observed[7], which may suggest that cationic rotational mobility influences the dielectric properties of the MHP, whilst incorporating cation reorientations when modelling the dielectric function have lowered estimates of the exciton binding energy from 40—50 meV[76] ($\epsilon_r \approx 6$) to as low as 2 meV ($\epsilon_r \approx 70$). A recent THz study by Davies *et al.* found that the exciton binding energies of $FAPbI_3$ and $MAPbI_3$ differ significantly, suggesting that the cation plays a significant role in modulation of the dielectric function and thus the exciton binding energy[77]. However, a magneto-optical study performed by Galkowski *et al.* found the change in

binding energy moving from $MAPbI_3$ to $FAPbI_3$ to be very small (~2 meV). Further studies will be necessary to ascertain the significance of cation rotations in dictating binding energies of of MHPs[78].

Theoretical[79] and experimental[61,62], studies suggest that the dynamics of the organic sublattice may also aid in the dissociation of bound carrier states. The same cation-driven dielectric relaxation discussed above has also been proposed to 'solvate' free carriers, resulting in a 'dielectric drag' effect that slows charge transport[80]. Additionally, Zhu *et al.* proposed that cation rotations may reduce scattering and suppress recombination[16], with others further suggesting that electrostatic fluctuations within the lattice resulting from dynamic disorder of the organic cation may spatially segregate electrons and holes[15,17]. An isotopic substitution study by Gong *et al.* suggests that decreasing the rotational rate of the MA^+ cation reduces carrier lifetimes, pointing to solvation effects like those proposed by Zhu *et al.* to explain their findings[63]. However, several experimental studies have identified little difference in charge transport behaviour for MHPs containing different cation compositions, suggesting that cation rotations do not strongly influence carrier dynamics. For example, a comparative study of $MAPbBr_3$ and $CsPbBr_3$ found that $CsPbBr_3$ was able to achieve a similar V_{OC} value (related to recombination losses) to that of $MAPbBr_3$[81]. Zhu *et al.* utilised transient photoluminescence (TRPL) spectroscopy and transient reflectance spectroscopy to compare several important parameters (including radiative and trap-assisted rate constants, surface recombination velocity, and surface carrier mobility) for, $MAPbBr_3$, $FAPbBr_3$, and $CsPbBr_3$ single crystals, finding that the organic cation had little effect on carrier recombination rates[82]. Additionally, similarities in recombination rates have also been observed for $CsPbBI_3$ and $MAPbI_3$, using transient THz spectroscopy[83]. Collectively, these results suggest that the organic cation is not essential to explain the low electron hole recombination rates in perovskite solar cells. It has been proposed (for example, in a recent AIMD study by Uratani and Yamashita[84]) that fluctuations in the inorganic PbI_3 sublattice instead may be the predominant factor in dictating recombination dynamics, potentially obviating the need to invoke cation rotations to rationalise carrier dynamics.

Whilst the relevance of organic cation in recombination processes remain unclear, there is experimental evidence that demonstrates that cation reorientations may influence hot carrier cooling. Hot carrier cooling is of significant interest in photovoltaics as it represents a significant loss pathway in all photovoltaic devices. Guo *et al.* made use of ultrafast microscopy directly probe the diffusion of hot carriers, finding diffusion lengths of approximately 600 nm, meaning that hot carriers could potentially be harvested before completely thermalizing[85]. This could possibly allow MHPs to achieve efficiencies above the 33% limit imposed by Shockley Quessier detailed balance. Several studies have provided indirect evidence that these relatively long hot carrier diffusion lengths arise due to rotations of the organic cations, including observations of trends in carrier cooling for different A-site cations[37] and reduction in carrier cooling upon intercalation of water[86]. Others have suggested the emergence of a phonon bottleneck due to acoustical phonon recycling[68,87] and/or restricted downconversion of LO phonons to acoustical phonons[69,88]. A recent study by Hopper *et al.*, utilising ultrafast pump-push-probe spectroscopy, indicates that the number of optical phonon modes predominantly dictates hot-carrier thermalisation rates[89].

Conclusions & Outlook. In this perspective, we have aimed to provide a comprehensive account of the current state of understanding of the dynamics of organic cations in MHPs. By attributing cation rotational lifetimes measured using different experimental techniques to different rotational regimes, we have shown that the wide range of rotational lifetimes within the literature are potentially reconcilable. Observations of surface ferroelectricity mean that further research is needed to elucidate how cation rotations differ in the bulk *versus* near surfaces/interfaces. Insight into cation

dynamics close to interfaces may be gleaned through computational techniques (*e.g.: ab initio* MD) or by experimentally investigating materials of differing morphologies.

The coupling between lattice dynamics and cationic rotations also appears to be significant at temperatures relevant to device performance. 2DIR results suggest that lattice vibrations directly drive cation reorientation, whilst the dynamic disorder of the cation distorts the inorganic sublattice, resulting in complex coupling between their dynamics. This interplay between motions of the organic and inorganic sublattice may influence material properties in ways that are relevant to device performance, such as in charge dynamics, and current-voltage hysteresis. Further investigation into cation rotations and cation-rotational coupling is essential to improve both the performance and technological applicability of these materials.

ACKNOWLEDGMENT

We thank Tom Hopper for useful discussions. A.A.B. is a Royal Society University Research Fellow. R.L. thanks the BMBF for funding (FKZ 13N13656). This project has also received funding from the European Research Council (ERC) under the European Union's Horizon 2020 research and innovation programme (grant agreement No 639750).

References

(1) Yang, W. S.; Park, B. W.; Jung, E. H.; Jeon, N. J.; Kim, Y. C.; Lee, D. U.; Shin, S. S.; Seo, J.; Kim, E. K.; Noh, J. H.; et al. Iodide Management in Formamidinium-Lead-Halide-Based Perovskite Layers for Efficient Solar Cells. *Science (80-.).* **2017**, *356* (6345), 1376–1379.

(2) Stranks, S. D.; Snaith, H. J. Metal-Halide Perovskites for Photovoltaic and Light-Emitting Devices. *Nat. Nanotechnol.* **2015**, *10* (5), 391–402.

(3) He, Y.; Galli, G. Perovskites for Solar Thermoelectric Applications: A First Principle Study of CH $_3$ NH $_3$ AI $_3$ (A = Pb and Sn). *Chem. Mater.* **2014**, *26* (18), 5394–5400.

(4) Zhang, Q.; Su, R.; Du, W.; Liu, X.; Zhao, L.; Ha, S. T.; Xiong, Q. Advances in Small Perovskite-Based Lasers. *Small Methods* **2017**, *1* (9), 1700163.

(5) Liu, D.; Lin, Q.; Zang, Z.; Wang, M.; Wangyang, P.; Tang, X.; Zhou, M.; Hu, W. Flexible All-Inorganic Perovskite CsPbBr $_3$ Nonvolatile Memory Device. *ACS Appl. Mater. Interfaces* **2017**, *9* (7), 6171–6176.

(6) Whitfield, P. S.; Herron, N.; Guise, W. E.; Page, K.; Cheng, Y. Q.; Milas, I.; Crawford, M. K. Structures, Phase Transitions and Tricritical Behavior of the Hybrid Perovskite Methyl Ammonium Lead Iodide. *Sci. Rep.* **2016**, *6* (1), 35685.

(7) Poglitsch, A.; Weber, D. Dynamic Disorder in Methylammoniumtrihalogenoplumbates (II) Observed by Millimeter-wave Spectroscopy. *J. Chem. Phys.* **1987**, *87* (11), 6373–6378.

(8) Eames, C.; Frost, J. M.; Barnes, P. R. F.; O'Regan, B. C.; Walsh, A.; Islam, M. S. Ionic Transport in Hybrid Lead Iodide Perovskite Solar Cells. *Nat. Commun.* **2015**, *6* (1), 7497.

(9) Even, J.; Pedesseau, L.; Jancu, J.-M.; Katan, C. Importance of Spin–Orbit Coupling in Hybrid Organic/Inorganic Perovskites for Photovoltaic Applications. *J. Phys. Chem. Lett.* **2013**, *4* (17), 2999–3005.

(10) Kieslich, G.; Sun, S.; Cheetham, A. K. An Extended Tolerance Factor Approach for Organic-Inorganic Perovskites. *Chem. Sci.* **2015**, *6* (6), 3430–3433.

(11) Fujiwara, H.; Kato, M.; Tamakoshi, M.; Miyadera, T.; Chikamatsu, M. Optical Characteristics

and Operational Principles of Hybrid Perovskite Solar Cells. *Phys. Status Solidi* **2018**, *215* (12), 1700730.

(12) Bernard, G. M.; Wasylishen, R. E.; Ratcliffe, C. I.; Terskikh, V.; Wu, Q.; Buriak, J. M.; Hauger, T. Methylammonium Cation Dynamics in Methylammonium Lead Halide Perovskites: A Solid-State NMR Perspective. *J. Phys. Chem. A* **2018**, *122* (6), 1560–1573.

(13) Mattoni, A.; Filippetti, A.; Saba, M. I.; Delugas, P. Methylammonium Rotational Dynamics in Lead Halide Perovskite by Classical Molecular Dynamics: The Role of Temperature. *J. Phys. Chem. C* **2015**, *119* (30), 17421–17428.

(14) Frost, J. M.; Butler, K. T.; Walsh, A. Molecular Ferroelectric Contributions to Anomalous Hysteresis in Hybrid Perovskite Solar Cells. *APL Mater.* **2014**, *2* (2), 81506–173502.

(15) Quarti, C.; Mosconi, E.; De Angelis, F. Structural and Electronic Properties of Organo-Halide Hybrid Perovskites from Ab Initio Molecular Dynamics. *Phys. Chem. Chem. Phys.* **2015**, *17* (14), 9394–9409.

(16) Zhu, X. Y.; Podzorov, V. Charge Carriers in Hybrid Organic-Inorganic Lead Halide Perovskites Might Be Protected as Large Polarons. *Journal of Physical Chemistry Letters*. American Chemical Society December 3, 2015, pp 4758–4761.

(17) Ma, J.; Wang, L.-W. Nanoscale Charge Localization Induced by Random Orientations of Organic Molecules in Hybrid Perovskite $CH_3NH_3PbI_3$. *Nano Lett.* **2015**, *15* (1), 248–253.

(18) Bechtel, J. S.; Seshadri, R.; Van Der Ven, A. Energy Landscape of Molecular Motion in Cubic Methylammonium Lead Iodide from First-Principles. *J. Phys. Chem. C* **2016**, *120* (23), 12403–12410.

(19) Taylor, V. C. A.; Tiwari, D.; Duchi, M.; Donaldson, P. M.; Clark, I. P.; Fermin, D. J.; Oliver, T. A. A. Investigating the Role of the Organic Cation in Formamidinium Lead Iodide Perovskite Using Ultrafast Spectroscopy. *J. Phys. Chem. Lett.* **2018**, *9* (4), 895–901.

(20) Weller, M. T.; Weber, O. J.; Frost, J. M.; Walsh, A. Cubic Perovskite Structure of Black Formamidinium Lead Iodide, α-$[HC(NH_2)_2]PbI_3$, at 298 K. *J. Phys. Chem. Lett.* **2015**, *6* (16), 3209–3212.

(21) Kanno, S.; Imamura, Y.; Saeki, A.; Hada, M. Rotational Energy Barriers and Relaxation Times of the Organic Cation in Cubic Methylammonium Lead/Tin Halide Perovskites from First Principles. *J. Phys. Chem. C* **2017**, *121* (26), 14051–14059.

(22) Lahnsteiner, J.; Kresse, G.; Kumar, A.; Sarma, D. D.; Franchini, C.; Bokdam, M. Room-Temperature Dynamic Correlation between Methylammonium Molecules in Lead-Iodine Based Perovskites: An Ab Initio Molecular Dynamics Perspective. *Phys. Rev. B* **2016**, *94* (21).

(23) Zhang, X.; Zhang, M.; Lu, G. Charge Stripe Formation in Molecular Ferroelectric Organohalide Perovskites for Efficient Charge Separation. *J. Phys. Chem. C* **2016**, *120* (42), 23969–23975.

(24) Shimamura, K.; Hakamata, T.; Shimojo, F.; Kalia, R. K.; Nakano, A.; Vashishta, P. Rotation Mechanism of Methylammonium Molecules in Organometal Halide Perovskite in Cubic Phase: An Ab Initio Molecular Dynamics Study. *J. Chem. Phys.* **2016**, *145* (22), 224503–144702.

(25) Meloni, S.; Moehl, T.; Tress, W.; Franckevičius, M.; Saliba, M.; Lee, Y. H.; Gao, P.; Nazeeruddin, M. K.; Zakeeruddin, S. M.; Rothlisberger, U.; et al. Ionic Polarization-Induced Current–voltage Hysteresis in CH3NH3PbX3 Perovskite Solar Cells. *Nat. Commun.* **2016**, *7*, 10334.

(26) Carignano, M. A.; Kachmar, A.; Hutter, J. Thermal Effects on CH 3 NH 3 PbI 3 Perovskite from Ab Initio Molecular Dynamics Simulations. *J. Phys. Chem. C* **2015**, *119* (17), 8991–8997.

(27) Goehry, C.; Nemnes, G. A.; Manolescu, A. Collective Behavior of Molecular Dipoles in $CH_3NH_3PbI_3$. *J. Phys. Chem. C* **2015**, *119* (34), 19674–19680.

(28) Mattoni, A.; Filippetti, A.; Caddeo, C. Modeling Hybrid Perovskites by Molecular Dynamics. *J. Phys. Condens. Matter* **2017**, *29*, 043001.

(29) Zhou, L.; Neukirch, A. J.; Vogel, D. J.; Kilin, D. S.; Pedesseau, L.; Carignano, M. A.; Mohite, A. D.; Even, J.; Katan, C.; Tretiak, S. Density of States Broadening in $CH_3NH_3PbI_3$ Hybrid Perovskites Understood from Ab Initio Molecular Dynamics Simulations. *ACS Energy Lett.* **2018**, 787–793.

(30) Whalley, L. D.; Frost, J. M.; Jung, Y.-K.; Walsh, A. Perspective: Theory and Simulation of Hybrid Halide Perovskites. *J. Chem. Phys.* **2017**, *146* (22), 220901.

(31) Bakulin, A. A.; Selig, O.; Bakker, H. J.; Rezus, Y. L. A.; Müller, C.; Glaser, T.; Lovrincic, R.; Sun, Z.; Chen, Z.; Walsh, A.; et al. Real-Time Observation of Organic Cation Reorientation in Methylammonium Lead Iodide Perovskites. *J. Phys. Chem. Lett.* **2015**, *6* (18), 3663–3669.

(32) Leguy, A. M. A.; Frost, J. M.; McMahon, A. P.; Sakai, V. G.; Kockelmann, W.; Law, C.; Li, X.; Foglia, F.; Walsh, A.; O'Regan, B. C.; et al. The Dynamics of Methylammonium Ions in Hybrid Organic–inorganic Perovskite Solar Cells. *Nat. Commun.* **2015**, *6* (1), 7124.

(33) Selig, O.; Sadhanala, A.; Müller, C.; Lovrincic, R.; Chen, Z.; Rezus, Y. L. A.; Frost, J. M.; Jansen, T. L. C.; Bakulin, A. A. Organic Cation Rotation and Immobilization in Pure and Mixed Methylammonium Lead-Halide Perovskites. *J. Am. Chem. Soc.* **2017**, *139* (11), 4068–4074.

(34) Wasylishen, R. E.; Knop, O.; Macdonald, J. B. Cation Rotation in Methylammonium Lead Halides. *Solid State Commun.* **1985**, *56* (7), 581–582.

(35) Onoda-Yamamuro, N.; Matsuo, T.; Suga, H. Calorimetric and IR Spectroscopic Studies of Phase Transitions in Methylammonium Trihalogenoplumbates (II)†. *J. Phys. Chem. Solids* **1990**, *51* (12), 1383–1395.

(36) Chen, T.; Foley, B. J.; Ipek, B.; Tyagi, M.; Copley, J. R. D.; Brown, C. M.; Choi, J. J.; Lee, S.-H. Rotational Dynamics of Organic Cations in the CH 3 NH 3 PbI 3 Perovskite. *Phys. Chem. Chem. Phys.* **2015**, *17* (17), 31278–31286.

(37) Zhu, H.; Miyata, K.; Fu, Y.; Wang, J.; Joshi, P. P.; Niesner, D.; Williams, K. W.; Jin, S.; Zhu, X. Y. Screening in Crystalline Liquids Protects Energetic Carriers in Hybrid Perovskites. *Science (80-.).* **2016**, *353* (6306), 1409–1413.

(38) Mcmorrow, D.; Lotshaw, W. T.; Kenney-Wallace, G. A. Femtosecond Optical Kerr Studies on the Origin of the Nonlinear Responses in Simple Liquids. *IEEE J. Quantum Electron.* **1988**, *24* (2), 443–454.

(39) Lee, J. H.; Bristowe, N. C.; Bristowe, P. D.; Cheetham, A. K. Role of Hydrogen-Bonding and Its Interplay with Octahedral Tilting in CH3NH3PbI3. *Chem. Commun.* **2015**, *51* (29), 6434–6437.

(40) Leguy, A. M. A.; Goñi, A. R.; Frost, J. M.; Skelton, J.; Brivio, F.; Rodríguez-Martínez, X.; Weber, O. J.; Pallipurath, A.; Alonso, M. I.; Campoy-Quiles, M.; et al. Dynamic Disorder, Phonon Lifetimes, and the Assignment of Modes to the Vibrational Spectra of Methylammonium Lead Halide Perovskites. *Phys. Chem. Chem. Phys.* **2016**, *18* (39), 27051–27066.

(41) Sendner, M.; Nayak, P. K.; Egger, D. A.; Beck, S.; Müller, C.; Epding, B.; Kowalsky, W.; Kronik, L.; Snaith, H. J.; Pucci, A.; et al. Optical Phonons in Methylammonium Lead Halide Perovskites

and Implications for Charge Transport. *Mater. Horizons* **2016**, *3* (6), 613–620.

(42) Niemann, R. G.; Kontos, A. G.; Palles, D.; Kamitsos, E. I.; Kaltzoglou, A.; Brivio, F.; Falaras, P.; Cameron, P. J. Halogen Effects on Ordering and Bonding of CH3NH3+in CH3NH3PbX3(X = Cl, Br, I) Hybrid Perovskites: A Vibrational Spectroscopic Study. *J. Phys. Chem. C* **2016**, *120* (5), 2509–2519.

(43) Svane, K. L.; Forse, A. C.; Grey, C. P.; Kieslich, G.; Cheetham, A. K.; Walsh, A.; Butler, K. T. How Strong Is the Hydrogen Bond in Hybrid Perovskites? *J. Phys. Chem. Lett* **2017**, *8*, 23.

(44) Ghosh, D.; Walsh Atkins, P.; Islam, M. S.; Walker, A. B.; Eames, C. Good Vibrations: Locking of Octahedral Tilting in Mixed-Cation Iodide Perovskites for Solar Cells. *ACS Energy Lett.* **2017**, *2* (10), 2424–2429.

(45) Kubicki, D. J.; Prochowicz, D.; Hofstetter, A.; Péchy, P.; Zakeeruddin, S. M.; Grätzel, M.; Emsley, L. Cation Dynamics in Mixed-Cation (MA)x(FA)1-XPbI3Hybrid Perovskites from Solid-State NMR. *J. Am. Chem. Soc.* **2017**, *139* (29), 10055–10061.

(46) Fabini, D. H.; Siaw, T. A.; Stoumpos, C. C.; Laurita, G.; Olds, D.; Page, K.; Hu, J. G.; Kanatzidis, M. G.; Han, S.; Seshadri, R. Universal Dynamics of Molecular Reorientation in Hybrid Lead Iodide Perovskites. *J. Am. Chem. Soc.* **2017**, *139* (46), 16875–16884.

(47) Zhang, D.; Zhu, Y.; Liu, L.; Ying, X.; Hsiung, C.-E.; Sougrat, R.; Li, K.; Han, Y. Atomic-Resolution Transmission Electron Microscopy of Electron Beam–sensitive Crystalline Materials. *Science (80-.).* **2018**, *359* (6376), 675–679.

(48) Röhm, H.; Leonhard, T.; Hoffmann, M. J.; Colsmann, A. Ferroelectric Domains in Methylammonium Lead Iodide Perovskite Thin-Films. *Energy Environ. Sci.* **2017**, *10* (4), 950–955.

(49) Xiao, Z.; Yuan, Y.; Shao, Y.; Wang, Q.; Dong, Q.; Bi, C.; Sharma, P.; Gruverman, A.; Huang, J. Giant Switchable Photovoltaic Effect in Organometal Trihalide Perovskite Devices. *Nat. Mater.* **2015**, *14* (2), 193–197.

(50) Coll, M.; Gomez, A.; Mas-Marza, E.; Almora, O.; Garcia-Belmonte, G.; Campoy-Quiles, M.; Bisquert, J. Polarization Switching and Light-Enhanced Piezoelectricity in Lead Halide Perovskites. *J. Phys. Chem. Lett.* **2015**, *6* (8), 1408–1413.

(51) Fan, Z.; Xiao, J.; Sun, K.; Chen, L.; Hu, Y.; Ouyang, J.; Ong, K. P.; Zeng, K.; Wang, J. Ferroelectricity of CH3NH3PbI3 Perovskite. *J. Phys. Chem. Lett.* **2015**, *6* (7), 1155–1161.

(52) Guzelturk, B.; Belisle, R. A.; Smith, M. D.; Bruening, K.; Prasanna, R.; Yuan, Y.; Gopalan, V.; Tassone, C. J.; Karunadasa, H. I.; McGehee, M. D.; et al. Terahertz Emission from Hybrid Perovskites Driven by Ultrafast Charge Separation and Strong Electron–Phonon Coupling. *Adv. Mater.* **2018**, *30* (11), 1704737.

(53) Rakita, Y.; Bar-Elli, O.; Meirzadeh, E.; Kaslasi, H.; Peleg, Y.; Hodes, G.; Lubomirsky, I.; Oron, D.; Ehre, D.; Cahen, D. Tetragonal CH 3 NH 3 PbI 3 Is Ferroelectric. *Proc. Natl. Acad. Sci.* **2017**, *114* (28), E5504–E5512.

(54) Pérez-Osorio, M. A.; Milot, R. L.; Filip, M. R.; Patel, J. B.; Herz, L. M.; Johnston, M. B.; Giustino, F. Vibrational Properties of the Organic–Inorganic Halide Perovskite $CH_3NH_3PbI_3$ from Theory and Experiment: Factor Group Analysis, First-Principles Calculations, and Low-Temperature Infrared Spectra. *J. Phys. Chem. C* **2015**, *119* (46), 25703–25718.

(55) Brivio, F.; Frost, J. M.; Skelton, J. M.; Jackson, A. J.; Weber, O. J.; Weller, M. T.; Goñi, A. R.; Leguy, A. M. A.; Barnes, P. R. F.; Walsh, A. Lattice Dynamics and Vibrational Spectra of the

Orthorhombic, Tetragonal, and Cubic Phases of Methylammonium Lead Iodide. *Phys. Rev. B* **2015**, *92* (14), 144308.

(56) Glaser, T.; Müller, C.; Sendner, M.; Krekeler, C.; Semonin, O. E.; Hull, T. D.; Yaffe, O.; Owen, J. S.; Kowalsky, W.; Pucci, A.; et al. Infrared Spectroscopic Study of Vibrational Modes in Methylammonium Lead Halide Perovskites. *J. Phys. Chem. Lett.* **2015**, *6* (15), 2913–2918.

(57) Yaffe, O.; Guo, Y.; Tan, L. Z.; Egger, D. A.; Hull, T.; Stoumpos, C. C.; Zheng, F.; Heinz, T. F.; Kronik, L.; Kanatzidis, M. G.; et al. Local Polar Fluctuations in Lead Halide Perovskite Crystals.

(58) Kabakova, I. V; Azuri, I.; Chen, Z.; Nayak, P.; Snaith, H. J.; Kronik, L.; Paterson, C.; Bakulin, A. A.; Egger, D. The Effect of Ionic Composition on Acoustic Phonon Speeds in Hybrid Perovskites from Brillouin Spectroscopy and Density Functional Theory. *J. Mater. Chem. C* **2018**, *6*, 3861.

(59) Grechko, M.; Bretschneider, S. A.; Vietze, L.; Kim, H.; Bonn, M. Vibrational Coupling between Organic and Inorganic Sub-Lattices of Hybrid Perovskites. *Angew. Chemie - Int. Ed.* **2018**.

(60) Kim, H.; Hunger, J.; Cánovas, E.; Karakus, M.; Mics, Z.; Grechko, M.; Turchinovich, D.; Parekh, S. H.; Bonn, M. Direct Observation of Mode-Specific Phonon-Band Gap Coupling in Methylammonium Lead Halide Perovskites. *Nat. Commun.* **2017**, *8* (1).

(61) D'Innocenzo, V.; Grancini, G.; Alcocer, M. J. P.; Kandada, A. R. S.; Stranks, S. D.; Lee, M. M.; Lanzani, G.; Snaith, H. J.; Petrozza, A. Excitons versus Free Charges in Organo-Lead Tri-Halide Perovskites. *Nat. Commun.* **2014**, *5*.

(62) Grancini, G.; Srimath Kandada, A. R.; Frost, J. M.; Barker, A. J.; De Bastiani, M.; Gandini, M.; Marras, S.; Lanzani, G.; Walsh, A.; Petrozza, A. Role of Microstructure in the Electron-Hole Interaction of Hybrid Lead Halide Perovskites. *Nat. Photonics* **2015**, *9* (10), 695–701.

(63) Gong, J.; Yang, M.; Ma, X.; Schaller, R. D.; Liu, G.; Kong, L.; Yang, Y.; Beard, M. C.; Lesslie, M.; Dai, Y.; et al. Electron–Rotor Interaction in Organic–Inorganic Lead Iodide Perovskites Discovered by Isotope Effects. *J. Phys. Chem. Lett.* **2016**, *7* (15), 2879–2887.

(64) Mosconi, E.; De Angelis, F. Mobile Ions in Organohalide Perovskites: Interplay of Electronic Structure and Dynamics. *ACS Energy Lett.* **2016**, *1* (1), 182–188.

(65) Tong, C.-J.; Geng, W.; Prezhdo, O. V; Liu, L.-M. Role of Methylammonium Orientation in Ion Diffusion and Current−Voltage Hysteresis in the CH 3 NH 3 PbI 3 Perovskite.

(66) Wright, A. D.; Verdi, C.; Milot, R. L.; Eperon, G. E.; Pérez-Osorio, M. A.; Snaith, H. J.; Giustino, F.; Johnston, M. B.; Herz, L. M. Electron-Phonon Coupling in Hybrid Lead Halide Perovskites. *Nat. Commun.* **2016**, *7*.

(67) Lin, Q.; Armin, A.; Nagiri, R. C. R.; Burn, P. L.; Meredith, P. Electro-Optics of Perovskite Solar Cells. *Nat. Photonics* **2015**, *9* (2), 106–112.

(68) Yang, J.; Wen, X.; Xia, H.; Sheng, R.; Ma, Q.; Kim, J.; Tapping, P.; Harada, T.; Kee, T. W.; Huang, F.; et al. Acoustic-Optical Phonon up-Conversion and Hot-Phonon Bottleneck in Lead-Halide Perovskites. *Nat. Commun.* **2017**, *8*, 14120.

(69) Monahan, D. M.; Guo, L.; Lin, J.; Dou, L.; Yang, P.; Fleming, G. R. Room-Temperature Coherent Optical Phonon in 2D Electronic Spectra of CH3NH3PbI3 Perovskite as a Possible Cooling Bottleneck. *J. Phys. Chem. Lett.* **2017**, *8* (14), 3211–3215.

(70) Unger, E. L.; Hoke, E. T.; Bailie, C. D.; Nguyen, W. H.; Bowring, A. R.; Heu, T.; Christoforo, M. G.; Mcgehee, M. D. Hysteresis and Transient Behavior in Current– Voltage Measurements of Hybrid-Perovskite Absorber Solar Cells.

(71) Yang, T. Y.; Gregori, G.; Pellet, N.; Grätzel, M.; Maier, J. The Significance of Ion Conduction in a Hybrid Organic-Inorganic Lead-Iodide-Based Perovskite Photosensitizer. *Angew. Chemie - Int. Ed.* **2015**, *54* (27), 7905–7910.

(72) Calado, P.; Telford, A. M.; Bryant, D.; Li, X.; Nelson, J.; O'Regan, B. C.; Barnes, P. R. F. Evidence for Ion Migration in Hybrid Perovskite Solar Cells with Minimal Hysteresis. *Nat. Commun.* **2016**, *7*, 13831.

(73) Huang, J.; Yuan, Y.; Shao, Y.; Yan, Y. Understanding the Physical Properties of Hybrid Perovskites for Photovoltaic Applications. *Nat. Rev. Mater.* **2017**, *2*, 17042.

(74) Pintilie, L.; Alexe, M. Ferroelectric-like Hysteresis Loop in Nonferroelectric Systems. *Appl. Phys. Lett.* **2005**, *87* (11), 112903.

(75) Scott, J. F. Ferroelectrics Go Bananas. *J. Phys. Condens. Matter* **2008**, *20* (2), 021001.

(76) Yang, Z.; Surrente, A.; Galkowski, K.; Bruyant, N.; Maude, D. K.; Haghighirad, A. A.; Snaith, H. J.; Plochocka, P.; Nicholas, R. J. Unraveling the Exciton Binding Energy and the Dielectric Constant in Single-Crystal Methylammonium Lead Triiodide Perovskite.

(77) Davies, C. L.; Borchert, J.; Xia, C. Q.; Milot, R. L.; Kraus, H.; Johnston, M. B.; Herz, L. M. Impact of the Organic Cation on the Optoelectronic Properties of Formamidinium Lead Triiodide. *J. Phys. Chem. Lett.* **2018**, 4502–4511.

(78) Galkowski, K.; Mitioglu, A.; Miyata, A.; Plochocka, P.; Portugall, O.; Eperon, G. E.; Wang, J. T.-W.; Stergiopoulos, T.; Stranks, S. D.; Snaith, H. J.; et al. Determination of the Exciton Binding Energy and Effective Masses for Methylammonium and Formamidinium Lead Tri-Halide Perovskite Semiconductors. *Energy Environ. Sci.* **2016**, *9* (3), 962–970.

(79) Hakamata, T.; Shimamura, K.; Shimojo, F.; Kalia, R. K.; Nakano, A.; Vashishta, P. The Nature of Free-Carrier Transport in Organometal Halide Perovskites. *Sci. Rep.* **2016**, *6*.

(80) Bonn, M.; Miyata, K.; Hendry, E.; Zhu, X. Y. Role of Dielectric Drag in Polaron Mobility in Lead Halide Perovskites. *ACS Energy Letters*. 2017, pp 2555–2562.

(81) Kulbak, M.; Cahen, D.; Hodes, G. How Important Is the Organic Part of Lead Halide Perovskite Photovoltaic Cells? Efficient CsPbBr3 Cells. *J. Phys. Chem. Lett.* **2015**, *6* (13), 2452–2456.

(82) Zhu, H.; Trinh, M. T.; Wang, J.; Fu, Y.; Joshi, P. P.; Miyata, K.; Jin, S.; Zhu, X.-Y. Organic Cations Might Not Be Essential to the Remarkable Properties of Band Edge Carriers in Lead Halide Perovskites. *Adv. Mater.* **2017**, *29* (1), 1603072.

(83) Dastidar, S.; Li, S.; Smolin, S. Y.; Baxter, J. B.; Fafarman, A. T. Slow Electron−Hole Recombination in Lead Iodide Perovskites Does Not Require a Molecular Dipole.

(84) Uratani, H.; Yamashita, K. Inorganic Lattice Fluctuation Induces Charge Separation in Lead Iodide Perovskites: Theoretical Insights. *J. Phys. Chem. C* **2017**, *121* (48), 26648–26654.

(85) Guo, Z.; Wan, Y.; Yang, M.; Snaider, J.; Zhu, K.; Huang, L. Long-Range Hot-Carrier Transport in Hybrid Perovskites Visualized by Ultrafast Microscopy. *Science (80-.).* **2017**, *356*, 59–62.

(86) Aphrham, S.; Pan, Q.; Zaccarine, S. F.; Felter, K. M.; Thieme, J.; van den Nieuwenhuijzen, K. J. H.; ten Elshof, J. E.; Huijser, A. Effect of Water Addition during Preparation on the Early-Time Photodynamics of CH3NH3PbI3 Perovskite Layers. *ChemPhysChem* **2017**, *18* (23), 3320–3324.

(87) Hejda, B.; Kra´l, K. Hot-Electron Cooling and Second-Generation Phonons in Polar Semiconductors. *Phys. Rev. B* **1993**, *47* (23), 15554–15561.

(88) Wang, H.; Valkunas, L.; Cao, T.; Whittaker-Brooks, L.; Fleming, G. R. Coulomb Screening and Coherent Phonon in Methylammonium Lead Iodide Perovskites. *J. Phys. Chem. Lett.* **2016**, *7* (16), 3284–3289.

(89) Hopper, T. R.; Gorodetsky, A.; Frost, J. M.; Müller, C.; Lovrincic, R.; Bakulin, A. A. Ultrafast Intraband Spectroscopy of Hot-Carrier Cooling in Lead-Halide Perovskites. *ACS Energy Lett.* **2018**, 2199–2205.

Author Biographies:

Nathaniel Potocki Gallop received his MSci in Chemistry from Imperial College London in 2016. He is currently a Ph. D. student, specialising in ultrafast spectroscopy applied to optoelectronic devices under the supervision of Dr. Artem Bakulin.

Oleg Selig completed his Ph.D. in the group of Yves Rezus at the research institute AMOLF and he received his degree from the University of Amsterdam. His work focused on ultrasensitive nonlinear vibrational spectroscopy of complex molecular systems.

Giulia Giubertoni received her M.S. degree at "*Universitá degli Studi*" of Milan. She is currently a PhD student under the direction of H.J. Bakker at AMOLF.

Huib J. Bakker

Yves L.A. Rezus

Jarvist Frost

Thomas la Cour Jansen works on computational spectroscopy at the University of Groningen. His recent interests include the coherent multidimensional spectroscopy, quantum mechanical materials design, and ultrafast dynamics. More information is available at https://www.rug.nl/staff/t.l.c.jansen/

Robert Lovroncic

Artem A. Bakulin received his M.Sc. degree from Lomonosov Moscow State University and Ph.D. from the University of Groningen. He is currently a Royal Society University Research Fellow at Imperial College London, focusing on ultrafast spectroscopy of nanodevices and vibronic phenomena in organic materials.

For Table of Contents only